Journal of
Chemical Engineering and Catalysis

Research Open Access

Using Silica Nanocomposite Modified with Amino Groups for Effective Wastewater Treatment

Ahmed M Desouky[1*], Mohamed EA Ali[1] and Ahmed Shahat[2]

[1]Hydrogeochemistry department, Desert Research Center, Cairo, Egypt
[2]Department of Chemistry, Faculty of Science, Suez University, Suez, Egypt

***Corresponding author:** Ahmed M Desouky, Hydrogeochemistry department, Desert Research Center, Cairo, Egypt, Tel: +01117257728, E-mail: ahmeddesouky_27@hotmail.com

Received Date: July 10, 2021 **Accepted Date:** August 10, 2021 **Published Date:** August 12, 2021

Citation: Ahmed M Desouky (2022) Using Silica Nanocomposite Modified with Amino Groups for Effective Wastewater Treatment. J Chem Eng Catal 1: 1-10.

Abstract

Nanosilica modified with aminogroup is created for Cu (II) and Pb(II) adsorption. The microspheres were characterized by scanning electron microscope (SEM) and Fourier transform infrared spectroscopy (FTIR). Batch adsorption tests indicated that NH2-Si exhibited higher adsorption affinity toward Cu (II) and Pb(II). The Langmuir model could fit the adsorption isotherm very well with maximum adsorption capacity of 163.16 and 147.79 mg/g, respectively, implying that adsorption processes involved monolayer adsorption. Pb(II) and Cu(II) adsorption could be well described by the pseudo second-order kinetics model, and was found to be strongly dependent on pH. The Pb(II)- and Cu(II)-loaded microspheres were effectively desorbed using 0.01 mol/L HCl. NH2-Si have promise for use as adsorbents in the removal of Pb(II) and Cu(II) in wastewater treatment processes. Any how this study indicated that modified silica nanoparticles can be used in different conditions as an effective, usable and inexpensive adsorbent for the heavy metals removal in aqueous solutions which values are higher than the standard level.

Keywords: Heavy Metals; Adsorption; Treatment; Silica-Functionalization

Introduction

Water contamination caused by heavy-metal ions generated from alloys, pigments, electroplating, mining, metallurgical activities, nuclear power plant operations, aerospace industries, electrical contacts, printing, and the manufacture of paper, rubber, plastics, and batteries is a global problem receiving worldwide attention. The extended persistence of water contamination in biological systems and the tendency to bioaccumulate while moving up the food chain is a serious threat to human health, living resources, and ecological systems [1]. The increased use of heavy substances metals in industry has resulted in increased availability of metallic in natural water sources [2]. The toxicity of such metal ions arise due to their non- biodegradable nature thereby accumulating in the living cells and impairing the normal functions of various organs of living beings. Technologies like chemical precipitation, electrochemical separation, membrane separation, reverse osmosis, ion exchange and adsorption resins though effective for metal remediation, yet are not competitive in industrial application [3-16].

For the heavy metals removal process are used various conventional methods such as redox reactions, solvent extraction, chemical precipitation and filtration, reverse osmosis, electrochemical treatment methods, ion exchange and lime coagulation which are characterized by low removal yields and high cost of operation. In the past years the adsorption process using nanomaterials was studied as an alternative solution, materials such as magnetic oxides, polymers, ceramic, silica and derivatives of carbon have been developed for wastewater treatment [17]. Adsorption treatments have been extensively developed to remove heavy metals in aqueous environments due to their simplicity and high efficiency. Nanoparticles have shown remarkable potential as adsorbents because these materials have large surface areas for the adsorption of heavy metals [18-20]. Modified nanosilica particles is an ideal support for functional groups because it is an inorganic material, stable under acidic conditions and non-swelling, and has high mass exchange characteristics and very high thermal resistance [21]. The chemical modification of nanosilica has shown great promise in improving the efficiency of adsorption due to the increase of functional groups [22].

Experimental

All chemicals were utilized without further purification. For all experiments, Milli-Q water was utilized. Cetyltrimethylammonium bromide (CTAB) and tetraethyl orthosilicate (TEOS) were from Sigma-Aldrich.

Synthesis of mesoporous silica nanospheres

The synthesis of mesoporous silica products was achieved by the ammonia-catalyzed hydrolysis of TEOS in a mixed solvent of water, diethyl ether and acetone using CTAB as a template at room temperature as described before [23]. Typically, 0.5 g of CTAB was dissolved in 100 ml of Milli-Q water and stirred for 30 min, followed by adding 40 g of acetone and stirred for 30 min, then, we added 20 g diethyl ether. After vigorous stirring for 30 min, 2.5 gm of TEOS was added and stirred for more 30 min, followed by adding 1.5 g NH_3 (25 *wt.*%). The resulting gel was vigorous stirred in a closed vessel at room temperature for 24 h. The particles were collected by filtration, cleaned with deionized water and dried at 80 °C for 24 h. Then they were calcined from room temperature to 550 °C for 4 h. followed by heating at 550 °C for 8 h more.

Preparation of NH2-MS

silica microspheres were dispersed in a mixture of ethanol/DI water, followed by addition of ammonium hydroxide. 3-Aminopropyltrimethoxysilane was added under mild stirring and ultrasonication. After 24 hr reaction and being washed with ethanol and DI water three times each, NH2- MS were obtained.

Instruments

Small angle X-ray diffraction (SAXRD) patterns were obtained by using XPERT – PRO – PANalytical with monochromated CuKα (λ = 1.54060 Å), wide angle X-ray diffraction (WAXRD) patterns were measured by using Bruker D8 Discover diffractometer with monochromated CuKα (λ = 1.54178 Å) at 40 kV, and 45 mA. The adsorption/desorption isotherms were collected using Quantachrom Autosorb system at 77 K. Prior to analysis, the samples were outgassed at 80 °C for 24 h. The BET surface areas pore volume and pore size distribution were calculated from N_2 adsorption data. The pore size distributions were obtained using the adsorption branch of the nitrogen isotherms by applying the Barrett–Joyner–Halenda (BJH) method. Field emission scanning electron microscopy (FESEM) images were obtained with a Zeiss Leo Supra55 microscope. The samples for FESEM observations were observed without any metal coating. A high-resolution transmission electron microscope (HR-TEM, Tecnai G20, FEI, and Netherland) was used for imaging, crystal structure revelation, and elemental analysis.

Result and Discussion

The morphology and structure of mesoporous silica nanospheres(MSNs)

Mesoporous silica nanospheres were prepared in a basic solution at room temperature utilizing acetone, ethyl ether, and water as cosolvents and cetyltrimethylammonium bromide (CTAB) as a surfactant.The small angle X-ray diffraction (SAXRD) patterns of the calcined MSNs (Fig. 1A) demonstrate a strong diffraction with a 2θ value of 2.2°. As a result, this sample was MCM-41 analogs, however, with a worm-like structure [24+. The absence of the peak at 2θ = 4.0–5.0° in MSNs showed that the mesopores were less ordered. This was confirmed visually by the TEM pictures showed in Figure. 4. Wide edge X-ray diffraction (WAXRD) demonstrate a strong diffraction peak in the range of 17 to 30° 2θ (Figure. 1B), which revealed normal occasional varieties of the electronic density because of the long-range ordering of the pores in the material [25].

As indicated by nitrogen adsorption–desorption analysis, mesoporous silica nanospheres showed type IV, with a precarious adsorption step at relative pressure of p/p_o = 0.35 and a wide hysteresis loop at p/p_o = 0.5–1.0 (Figure 2A), comparing to a bimodal pore structure (Figure. 2B). The little pores with diameter of 3 nm are identical in the typical mesoporous silica templated by CTAB and, in this manner, doled out to the main channel of the composite, while, a large distribution of mesopores with diameters around 25 nm likewise appeared for the mesoporous silica nanosphere, inferring the dissolution of unnecessary ethyl ether into the micelle of CTAB to expand the pore of resulting sample, and lead to the decline of mesostructure simultaneously [24]. The N_2 isotherms portrayed in Figure 2A, (N_2 uptake) demonstrating the surface area of MSNs. The obvious Brunauer–Emmett–Teller (BET) surface area value of the parent MSNs (873.55 m^2g^{-1}). The pore volume of the MSNs (1.135 cm^3/g). The pore size distribution of the MSNs demonstrates a novel peak focused at around 3.83 nm diameters (Figure 2B).

FESEM of the MSNs (A) and MSNs-NH_2(B) samples is shown in Figure 3. Based on the FESEM observations, the material occurs as nanospheres.

The TEM images representative nanospheres of 700 nm in size (Figure 4), and large slitlike mesopores with the length of 20-50 *nm* are homogeneously distributed on the nanosphere surface. The contrast and distribution of dark and pale parts around the edge of nanosphere also indicate the existence of large radially oriented mesopores (Figure 4).

The SEM images representative nanospheres of MSNs and NH_2-MSNs show the particles of MSNs was stick together as shown in Figure.5(A). On the other hand, the SEM image of NH_2-MSNs particles embedded was depicted in Figure. 5(B) the distribution of highly porous characteristic of NH_2-MSNs particles on the surface is clearly shown. Thus surface pores increased the effective surface area of the nanocomposite as compared to the MSNs The functional groups present in silica and NH_2-silica hybrid materials were monitored by FT-IR spectroscopy.In Fig. 6 (B) shows that The Si-O bond exhibits peaks at 485 cm^{-1} and 3693 cm^{-1} is the NH stretching vibration peak of the amines. The stretching vibration peaks of Si-O-Si appear at 1062 cm^{-1} and 1347 cm^{-1}, and the asymmetry vibration peaks appear at 797 cm^{-1}; Si-OH has a symmetrical stretching vibration peak at 895 cm^{-1} the absorption band at 1635 cm^{-1} was attributed to the N-H bending vibrations The absorbance peaks corresponding to the C–H stretching and bending vibrations appear in 2205 and 2104 cm^{-1}; these peaks became intense in all material containing amine. attributed to the vibrations N–H of $–NH_3^+$. The presence of N–H bending vibration around 797 cm^{-1} and the symmetric –NH2 bending vibration confirm the incorporation of amino groups. The Si–OH vibration band decrease around 895 cm^{-1}

Effect of pH

The pH of a solution strongly affects the adsorption capacity of the modified silica. So the effect of solution pH on metal ions removal after socking of 24 hr. was studied at pH ranges of 2 - 5, by adjusting the solution pH using 0.1N HCl or 0.1N NaOH. It is important to mention that, modified silica is not stable at strong acidic medium, so its adsorption behavior was studied at pH ranges from 2-5.

Figure 7 shows the effect of pH on the individual adsorption of Cu (II) and Pb (II) by modified silica. The adsorption increases with increasing the pH value up to 5 where the maximum adsorption was obtained. The low adsorption of metal ions in strong acidic pH solution (at low pH) could be mainly due to the electrostatic repulsion between the positive metal ions (M^+) in the medium and the positive charges in highly acidic solution (H^+) which accumulate on the surface of modified silica. In the other words, the amino groups in modified silica is easily form protonation, reducing the number of binding sites available for the adsorption of heavy metal ions. This leads to the inducing an electrostatic repulsion of the different heavy metal ions. Therefore, the competition existed between protons and the metal ions (M^+) for adsorption sites and adsorption capacity was decreased. Such repulsion prevents the approach of the metal ions to modified silica surface.

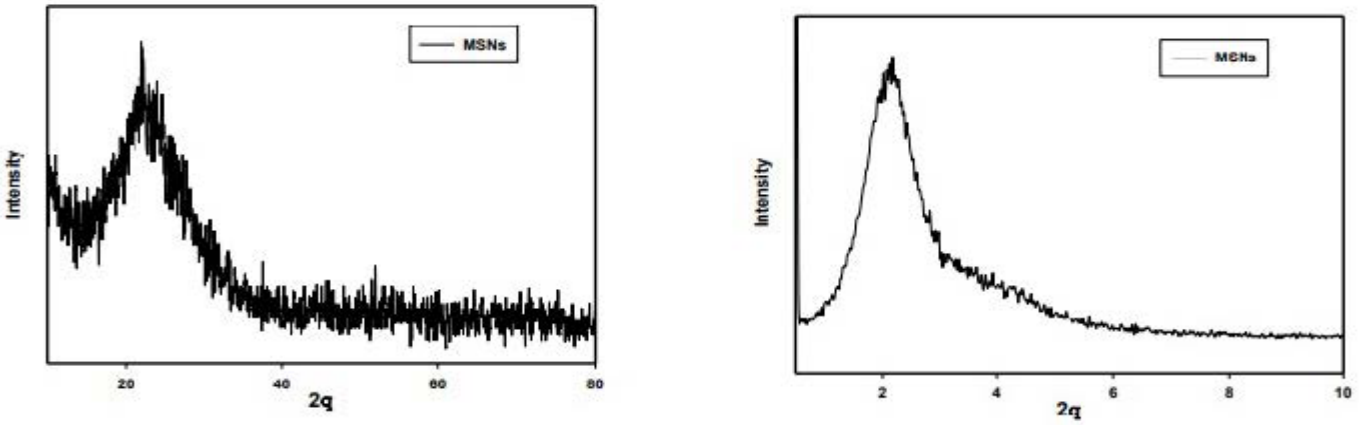

Figure 1: (A) Small-angle X-ray diffraction (SAXRD) patterns and (B) wide-angle XRD (WAXRD) patterns of the calcined MSNs.

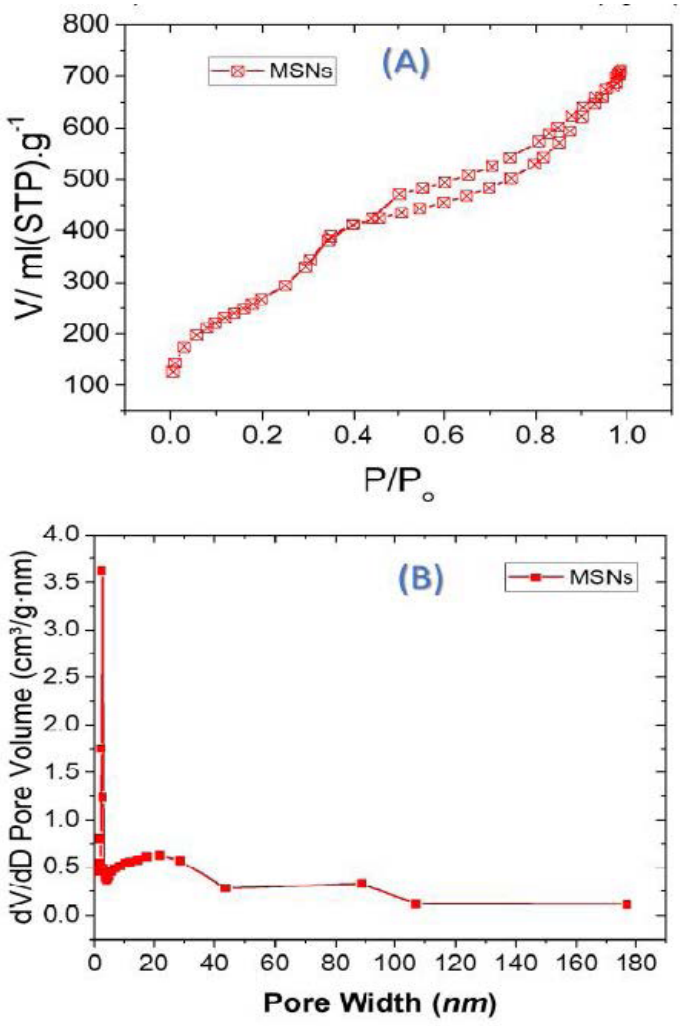

Figure 2: Nitrogen adsorption isotherms (A) and pore size distribution (B) of MSNs and the TMK sensor.

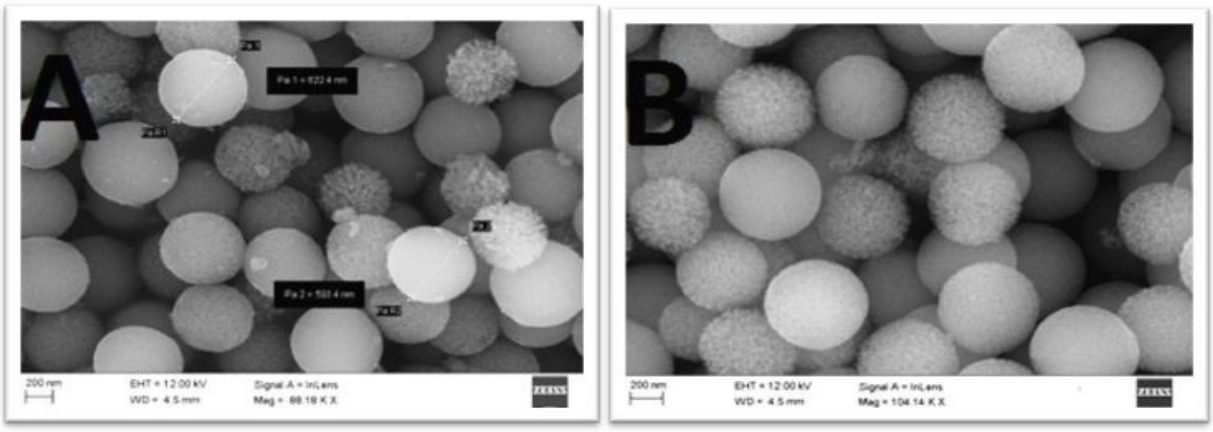

Figure 3: FESEM images of the MSNs(A) and MSNs-NH2(B)

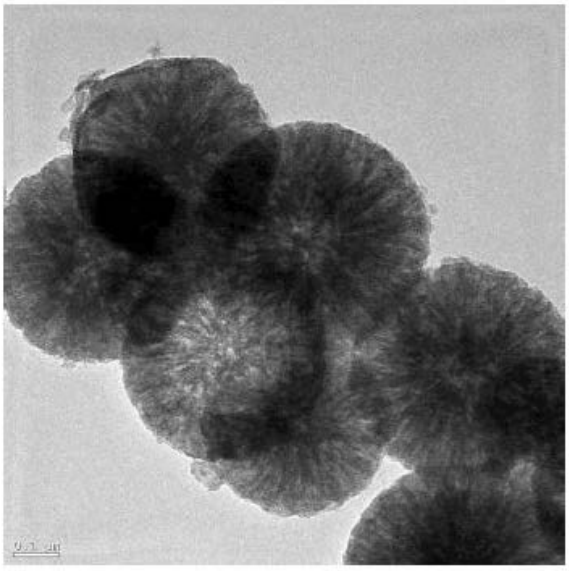

Figure 4: Representative TEM images of the MSNs

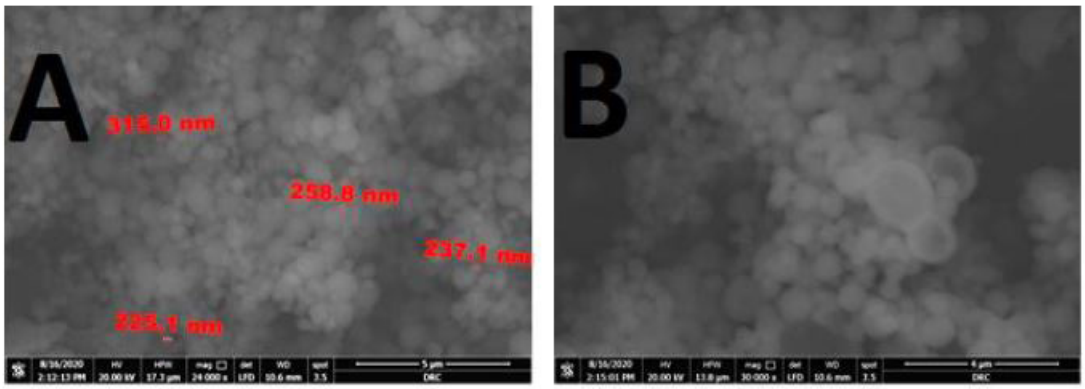

Figure 5: Scanning electron microscope images of MSNs (A) and NH2/ MSNs (B)

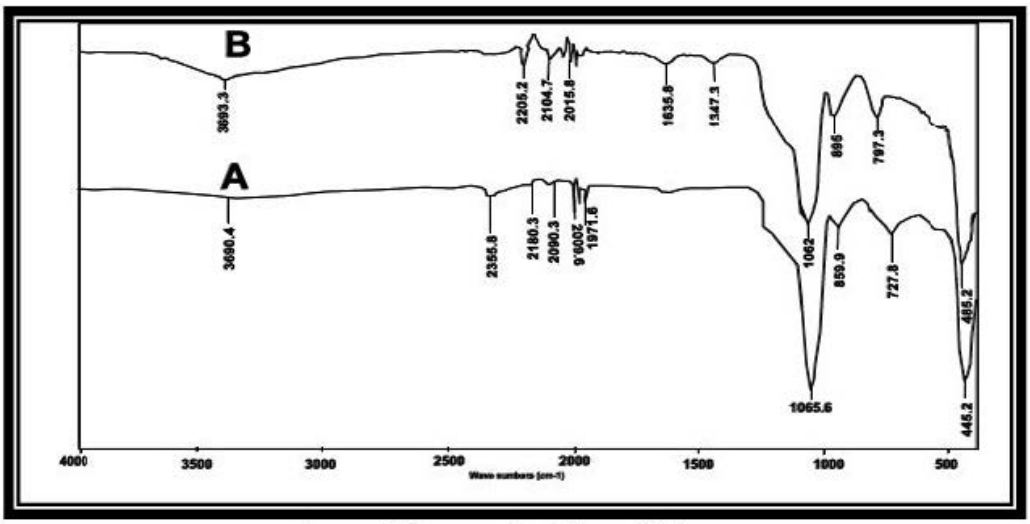

Figure 6: IR shows of the samples (A)Si and (B) NH2-MS

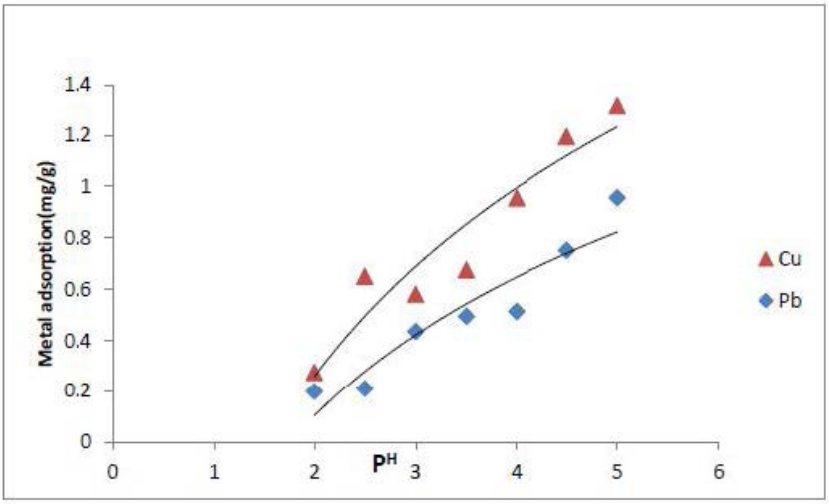

Figure 7: pH-dependent metal uptake of metal ion

While at higher pH value, the adsorption of heavy metal ions increases due to the weaker electrostatic repulsion, and with the increase of pH value, the amino groups are free from protonation. Such positive charge density decreases allowing the metal ions to approach the different sorbent beads surface which result in higher adsorption values. The adsorption mechanism may be partially replaced by a chelation mechanism on the amino groups of modified silica. Further increase in the pH value more than 5 would transform the dissolved metal into precipitated hydroxide form thus the adsorption capacity is decreased. This is well agreement with the previous works [26].

Effects of contact time

The effects of contact time on the removal of Cu(II) and Pb(II) by modified silica are depicted in Fig. 8. Initially the metal uptake was fast due to the many vacant adsorption sites, all the active sites were occupied by target Cu(II) or Pb(II) within 2hrs after which the adsorption rate gradually decreased and became constant at equilibrium to attain equilibrium conditions where the concentration of adsorbate in the bulk solution was in dynamic balance with that at the interface. It is possible that some of the adsorption sites of modified silica were easily obtained due to increases of the functional groups on its surface. This was also seen from the higher kinetics of copper adsorption by modified silica compared to lead ions. Due to the small increase of the adsorption capacity after 2hrs of mixing, contact time of 24 h was selected for all the equilibrium tests.

Adsorption kinetics

Modeling of adsorption kinetics was conducted by using the pseudo-first-order and pseudo- second-order models. These originally empirical models have been used extensively to describe the sorption kinetics.

The pseudo-first-order model is expressed as[26]:

$$\text{Log}\,(q_e - q_t) = \log q_e - k1/2.303\ t \quad (1)$$

The dependence from Cu (II) and Pb(II) adsorption onNH2-MS against contact time is shown in Figure 9.

The pseudo second-order model has usually been adopted to describe mass transfer processes. The pseudo-second-order rate equation is:

$$t/qt=(1/k2qe2)+1/qe\ t \quad (2)$$

where, qe (mg/g) is the adsorption amount at equilibrium, qt (mg/g) is the adsorption amount at time t, k_1 (min^{-1}) and k_2 ($gmg^{-1}\ min^{-1}$) are the pseudo- first-order and pseudo-second-order rate constants.Simulation results were obtained from Cu (II) and Pb(II) adsorption based on the pseudo second-order kinetics model. As shown in Figure. 10 pseudo second-order kinetics present a linear relation with R^2 higher than 0.98. Moreover, Cu (II) and Pb(II) adsorption amounts obtained from data (39.50 and 31 mg/g). while pseudo first- order kinetics present a linear relation with R^2 not more 0.95. Thus, Cu (II) and Pb(II) adsorption processes on NH2-MS obeyed pseudo second-order kinetics.The adsorption rate constants ofCu (II) and Pb(II) calculated based on the pseudo second order kinetics were 0.72 $\times 10^{-2}$ and 0.61×10^{-2} g/(mg·min).

There were two steps for the heavy metal adsorption by NH2-MS. First, a large amount of heavy metals was rapidly adsorbed by the exterior surface and amino groups of NH2-MS. When the adsorption of exterior surface reached saturation, heavy metals entered into the pores and were absorbed by the interior surface of NH2-MS. The fitted results are presented in Table 1.

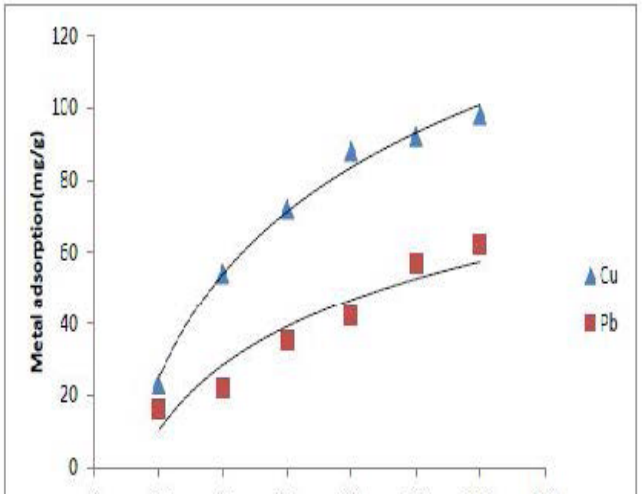

Figure 8: Metal uptake of metal ion with time

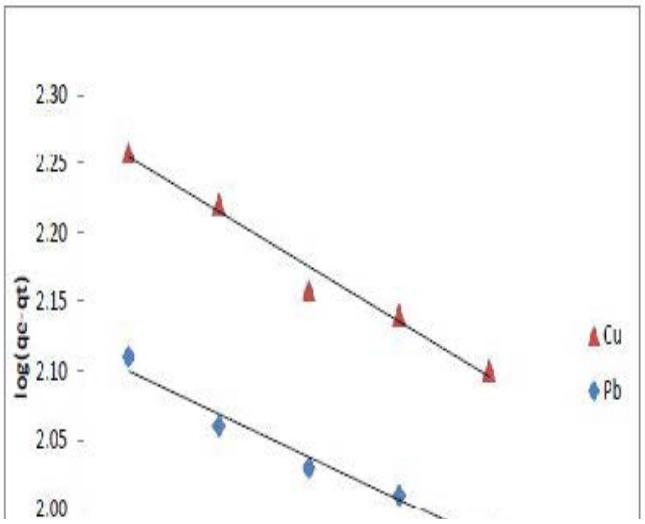

Figure 9: Plots of log(qe-qt) ainst time for the exchange of Cu (II) and Pb(II) ions on NH2-MS

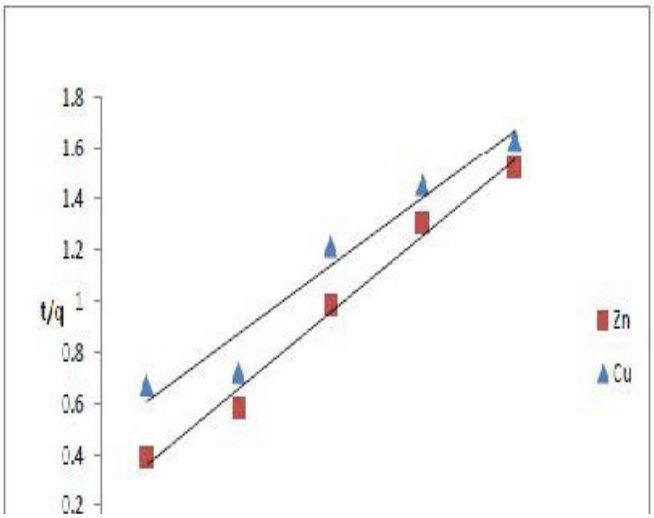

Figure 10: Pseudo second order model for the exchange of Cu (II) and Pb(II) ions on NH2-MS

pseudo first-order				pseudo second-order		
Metal Ions	qe,	$K_1 \times 10^{-2}$	R2	qe	$K_2 \times 10^{-2}$	R^2
Cu^{2+}	179	0.92	0.94	39.5	0.72	0.983
Pb^{2+}	172.5	0.72	0.95	31	0.61	0.985

Table. 1. Pseudo - First and second order parameters for the adsorption of Cu(II) and Pb(II) on NH2-MS.

Adsorption isotherms

The adsorption isotherm is important for determining the adsorption behavior of an adsorbent. The Cu (II) and Pb(II) adsorption isotherms of the NH2-MS were compared at pH 5. The maximum Cu (II) and Pb(II) adsorption amounts on NH2-MS within the tested concentration range were substantially enhanced by functionalization,as shown in Figures. 11,12 which was achieved through the complexation of metal ions by amino groups [27].

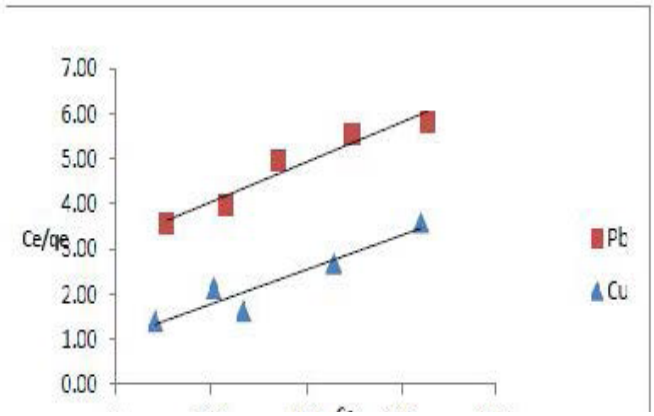

Figure 11: plot of (Ce/qe) ainst Ce for Cu (II) and Pb(II) metals ions

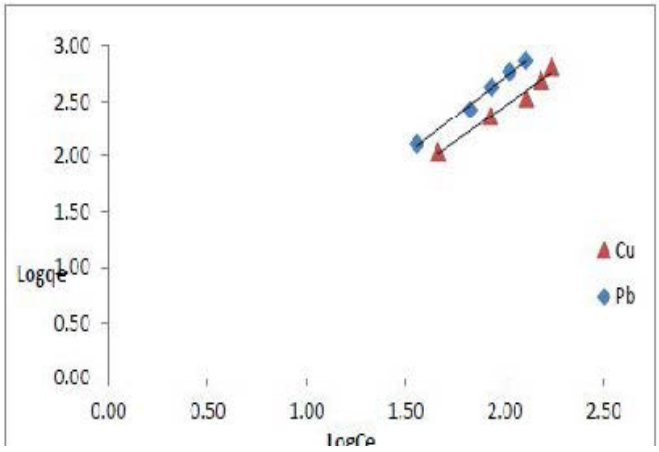

Figure 12: plot of log qe versus log Ce for Cu (II) and Pb(II) metals ions

The equilibrium data were fitted by the Langmuir (Eq. (3)) and Freundlich (Eq. (4)) models:

$$ce/qe = 1/Qob + 1/Qo\ ce \qquad (3)$$

$$\log qe = \log kf + (1/n) \log C \qquad (4)$$

where, *q*max (mg/g) is the theoretical maximum heavy metal adsorption amount, *q*e (mg/g) is the equilibrium adsorption amount at heavy metal equilibrium concentration *C*e (mg/L), *k*f is the Freundlich coefficient characteristic of the adsorption affinity of the adsorbent, and *n* is the linearity index. Langmuir and Freundlich equations are employed to describe the adsorption process in heterogeneous systems. The Langmuir models assume monolayer adsorption on the solid surface while Freundlich model is empirical in nature.The fitted results are presented in Table 2.

Metals	Langmuir constants (NH2-MS)			Freundlich constants (NH2-MS)		
	Q_{max} (mg/g)	KL	R^2	KF	1/n	R^2
Cu(II)	163.16	0.38	0.988	1.4	0.79	0.93
Pb(II)	147.79	0.44	0.989	1.2	0.71	0.92

Table 2

The results showed that the Langmuir model with R^2 higher than 0.98 fitted better than the Freundlich model, indicating that Cu (II) and Pb(II) adsorption on NH2-MS can be considered to be a monolayer adsorption process. The amino groups had a strong affinity towards metal ions, and the possible adsorption mechanism could be explained by the coordinate interactions [27] .In addition, all the Freundlich adsorption intensity variables supported the favorable adsorption of metal ions with NH2-MS. The adsorption capacities of Cu (II) and Pb(II) were 163.16 and 147.79 mg/g respectively. By comparison, the adsorption capacity of Cu(II) was higher than that of Pb(II), which could result in a higher utilization of amino groups in the adsorbent in Cu (II) adsorption, leading to its larger saturation adsorption capacity[27].

Adsorbent	q_m (mg/g)	Ref.
Silica-Activated Carbon	178.5	2
Metal oxide nanoparticles Fe_3O_4	127.4	3
Rice husk ash	39.87	4
Poly(ethyleneimine)-Functionalized Silica	36.8	21
NH2-MS	179	This study

Table 3 comparison of the maximum adsorption capacity of heavy metals onto different adsorbents.

Application

In the 10th of Ramadan, waste water contains heavy metals. From the chemical analysis of the five waste water samples it is clear that, the soluble heavy metals of waste water samples such as Lead is more than the permissible limit (0. 1 mg/l). To overcome this problem, two of waste water samples were chosen for the treatment process. The efficiency of the treatment was measured by chemical analysis samples before and after this process using NH2-MS. It was found that the soluble Lead in samples was 0.052 ppm before treatment and 0.09 ppm after treatment, and 0.03 ppm before treatment and 0.007 ppm after treatment. It can be concluded that the surfaces of NH2-MS had adsorption sites that were able to bind Cu(II) ions.

Conclusions

NH2-MS were found to effectively adsorb Cu(II) and Pb(II) from aqueous solutions. The maximum metal uptake by the NH2-MS were 147.79 and 163.16 mg/g for Pb(II) and Cu(II), respectively. The selectivity sequence of both ions uptake as follow; Cu(II)- NH2-MS > NH2- MSPb(II) were in accordance with the stability constants of the metal chelates of NH2-MS. Adsorption kinetics followed a pseudo-Second-order model for NH2-MS, but the rate of the adsorption was also affected by intraparticle diffusion. Modeling of adsorption equilibrium required not only the choice of isotherm equation but also the error function. The quality of the fit was judged by a few statistical tests as well as accurate approximation of the real adsorption capacity (qe). Langmuir model should better describe the two metal ions adsorption on aminated mesoporous materials than Freundlich model where the R^2 values are compared.

References

1. Marwa Nabil, Hussien A, Motaweh (2015) Porous Silicon Powder as an Adsorbent of Heavy Metal (Nickel): 1-21.

2. Mona Karnib, Ahmad Kabbani, Hanafy Holail, Zakia Olama (2014) Heavy Metals Removal Using Activated Carbon, Silica and Silica Activated Carbon Composite. ScienceDirect 50: 113–20.

3. Juttner K, Galla U, Schmieder H (2000) Electrochemical approaches to environmental problems in the process industry. Electrochim.Acta 45: 2575-94.

4. Yang XJ, Fane AG, McNaughton S (2001) Removal and recovery of heavy metals from wastewater by supported liquid membranes. Water Sci. Technol 43: 341-8.

5. Bose P, Bose MA, Kumar S (2002) Critical evaluation of treatment strategies involving adsorption and chelation for wastewater containing copper, zinc, and cyanide. Adv. Environ. Res 7: 179-95.

6. Wingenfelder U, Hansen C, Furrer G, Schulin R (2005) Removal of heavy metals from mine water by natural zeolites. Environ. Sci. Technol 39: 4606-13.

7. Dobrevsky I, Todorova-Dimova M, Panayotova T (1997) Electroplating rinse wastewater treatment by ion exchange. Desalination 108: 277-80.

8. Korngold E, Belayev N, Aronov L (2003) Removal of chromates from drinking water by anion exchangers. Sep. Purif. Technol 33: 179-87.

9. Ahmed S, Chughtai S, Keane MA (1998) The removal of cadmium and lead from aqueous solution by ion exchange with Na–Y zeolite. Sep. Purif. Technol 13: 57-64.

10. Cheng RC, Liang S, Wang HC, Beuhler MD (1994) Enhanced coagulation for arsenic removal. J. Am. Water Works Assoc 86: 79-90.

11. Edwards M (1994) Chemistry of arsenic removal during coagulation and Fe-Mn oxidation. J. Am. Water Works Assoc 86: 64-78.

12. Wang LK, Fahey EM, Wu ZC (2004) Dissolved air flotation. In: Wang LK, Hung YT, Shammas NK, eds. Physicochemical treatment processes. New Jersey: Humana Press 2004: 431-500.

13. Matis KA, Zouboulis AI, Gallios GP, Erwe T, Blöcher C (2004) Application of flotation for the separation of metal-loaded zeolite Chemosphere 55: 65-72.

14. Chakravarti AK, Chowdhury SB, Chakrabarty S, Chakrabarty T, Mukherjee DC (1995) Liquid membrane multiple emulsion process of chromium(VI) separation from wastewaters. Colloids Surf. A Physicochem. Eng. Aspects 103: 59-71.

15. Kongsricharoern N, Polprasert C (1996) Chromium removal by a bipolar electrochemical precipitation process. Water Sci.

Technol 34: 109-116.

16. Dabrowski A (2001) Adsorption - from theory to practice. Adv.Colloid Int Sci 93: 135-224.

17. CI Covaliu, G Paraschiv, O Stoian, A Vişan (2019) Nanomaterials applied for heavy metals removal from Wastewater Materials Science and Engineering 572: 012074

18. Chauhan N, Gupta S, Singh N, Singh S S, Islam S, et al. (2011) Aligned nanogold assisted one step sensing and removal of heavy metal ions. J Colloid and Interface Sci 363: 42–50.

19. Zhu H X, Jia S R, Wan T, Jia Y Y, Yang H J, et al (2011) Biosynthesis of spherical Fe3O4/bacterial cellulose nanocomposites as adsorbents for heavy metal ions. Carbohydrate Polymers 86: 1558–64.

20. Hua M, Zhang SJ, Pan BC, Zhang WM, Lv L, Zhang QX (2012) Heavy metal removal from water/wastewater by nanosized metal oxides: A review. J Hazardous Materials 211-212: 317–31.

21. Fan H, Fan X i, Li J, Guo M, Zhang D, et al. (2012) Selective Removal of Arsenic(V) from Aqueous Solution Using a Surface-Ion-Imprinted Amine-Functionalized Silica Gel Sorbent, Ind. Eng. Chem. Res 51: 5216-23.

22. Jal PK, Patel S, Mishra BK (2004) Chemical Modification of Silica Surface by Immobilization of Functional Groups for Extractive Concentration of Metal Ions Talanta 62: 1005-28.

23. A Shahat, S Trupp (2017) Sensitive, selective, and rapid method for optical recognition of ultra- traces level of Hg(II), Ag(I), Au(III), and Pd(II) in electronic wastes, Sensors and Actuators B Chemical 245: 789–802.

24. FN Gu, WG Lin, JY Yang, F Wei, Y Wang (2012) Fabrication of centimeter-sized sphere of mesoporous silica with well-defined hollow nanosphere topology and its high performance in adsorbing phenylalanine, Microporous and Mesoporous Materials 151: 142–8.

25. H Wanyika, E Gatebe, P Kioni, Z Tang, Y Gao (2011) Synthesis and characterization of ordered mesoporous silica nanoparticles with tunable physical properties by varying molar composition of reagents Afr. J. Pharm. Pharmacol 5: 2402-2410.

26. AM Desouky (2018) Remove heavy metals from groundwater using carbon nanotubes grafted with amino compound, Separation Science and Technol.

27. Yulin Tang, Song Liang, Juntao Wang, Shuili Yu, et al. (2013) Amino-functionalized core-shell magnetic mesoporous composite microspheres for Pb(II) and Cd(II) removal. J Environ Sci 25: 830–7.